ELSEVIER

Polymer 43 (2002) 3759–3766

polymer

www.elsevier.com/locate/polymer

Exfoliated and intercalated polyamide-imide nanocomposites with montmorillonite

Ajit Ranade, Nandika Anne D'Souza*, Bruce Gnade

Department of Materials Science, University of North Texas, P.O. Box 305310, Denton, TX 76203, USA

Received 7 August 2001; received in revised form 22 January 2002; accepted 24 January 2002

Abstract

Polyamide-imide (PAI) is a high performance condensation polymer, which has high heat resistance and high radiation resistance. Solvent suspensions of PAI are widely used in magnetic wire coatings. Montmorillonite (MMT) nanocomposites were investigated for the concentration effects on dispersion, glass transition, degradation, and mechanical properties. Samples were prepared using a controlled torque stirrer and slow solvent extraction was followed for the cast samples. Optical microscopy shows that the surface of the cast sample has increased edge–edge clay platelet attraction. Transmission electron microscopy of the through thickness sample indicated platelet edges, increased face–face coagulated states and some edge–edge flocculated states of tactoid formation. X-ray diffraction indicated that for 1% sample a highly exfoliated structure was obtained while between 1.5 and 3% intercalated and exfoliated dispersions were obtained. The glass transition was not significantly affected by clay presence but a drop in specific heat change was observed for all samples showing a 001 clay peak presence. The first heating scan showed PAI solvent and MMT organic emission but these emissions did not affect the PAI chemically. Degradation was altered by the level of matrix shielding by the clay. Hardness values were increased with clay presence but unaffected by concentration.

Keywords: Polyamide-imide; Montmorillonite; Nanocomposites

1. Introduction

When two or more phases are mixed together to make a composite, a combination of properties that are not available in any of the individual components is possible. There has been extensive interest in the development of polymer–clay nanocomposites from the earliest work involving nylon from scientists of Toyota Corporation [1–9]. The influence of clay treatment on dispersion [10–13] has driven much of the earlier research. Scientists have also tried to correlate and explain the behavior of nanocomposites through thermodynamic models to understand clay treatments and formation of nanocomposites [14–20]. Improved barrier properties [21–25], higher mechanical properties [26–30], improved flame retardancy [31–34], and increased dimensional stability [35–39] have been determined in polymer nanocomposites. All of these benefits are obtained without significantly raising the density of the compound or reducing light transmission [14]. The potential property enhancements have led to increased application in various fields such as the automobile industry (exterior and interior body parts and fuel tanks), packaging industry (bottles, containers, and plastic films), electronic industry (packaging material and exterior parts of electronic devices), coating industry (paints, wire enamel coatings, etc.), and aerospace industry (body parts of airplane and exterior surface coatings) [14,32,33,35].

The word 'nanocomposite' refers to composites whose reinforcement has at least one dimension in the nanometer scale [32,33]. Here the nanoscale filler is a pristine mica type layered silicate. Because the building blocks of nanocomposites are nanoscale (1 nm thick and 100–1000 nm in length), they have enormous surface area leading to a high interfacial area between filler and matrix. Special properties of the nanocomposite arise from the interactions at the interfaces. By contrast, in a conventional composite based on micrometer sized fillers such as carbon fibers and glass fibers, the interfaces between the filler and matrix constitute a much smaller volume fraction of the bulk material and therefore influence its properties to a much smaller extent.

To make a successful nanocomposite, it is very important to be able to disperse the inorganic material throughout the polymer. If a uniform dispersion is not achieved, agglomerates of inorganic material are found within the host polymer matrix, thus limiting improvement [12,14,36].

* Corresponding author. Tel.: +1-940-565-2979; fax: +1-940-565-4824.
E-mail address: ndsouza@unt.edu (N.A. D'Souza).

0032-3861/02/$ - see front matter
PII: S0032-3861(02)00106-4

Since montmorillonite (MMT) is a layered silicate, separation of the layers by intercalating polymer chains, or completely disrupting the layers, is vital to property improvement.

Factors limiting successful dispersion of the layered silicates are the hydrophilic nature of the silicates and the largely hydrophobic nature of most engineering polymers. To produce an intercalated nanocomposite, the polymer has to wet the clay particles to some extent so that the polymer chains are intercalated between the clay galleries. To make delaminated or exfoliated nanocomposites, a higher degree of wetting is required [11,12,14,23,28,30].

To enhance polymer–clay interaction, the clay interlayer surfaces of the silicate are chemically treated to make the silicate less hydrophilic and therefore more wettable by the polymer. A cation exchange process accomplishes this where hydrophilic cations such as Na^+, K^+, and Ca^{2+} are exchanged by alkyl ammonium cations. The role of alkyl ammonium cations in the organosilicates is to lower the surface energy of the inorganic host and improve the wetting characteristics with the polymer. The length of the alkyl ammonium cations determines the hydrophobicity of silicate layers [14].

Polyamide-imide (PAI) is a high performance condensation polymer, which has high heat resistance. Suspensions of PAI are widely used in magnetic wire coatings in under-the-hood automotive applications. Increasing the glass transition temperature with retention of PAI thermo-oxidative stability and mechanical performance leads to increased reliability and service lifetimes.

The objective of this paper is to investigate PAI + MMT nanocomposites. The role of MMT concentration on the state of dispersion was determined using optical microscopy (OM), X-ray diffraction (XRD), and transmission electron microscopy (TEM). The influence of MMT concentration on the glass transition (T_g) was determined using differential scanning calorimetry (DSC). The results were correlated to the state of dispersion based on the influence of chain confinement. Since the MMT is treated organically with alkyl ammonium surfactants having a degradation temperature of 270 °C, thermogravimetric analysis (TGA) was conducted to determine how the high PAI degradation temperature was affected by surfactant degradation. The influence of MMT on the mechanical properties was determined through Vickers hardness measurements. The results indicate that MMT concentration affects the state of dispersion, which has a dominating influence on the degradation and mechanical properties.

2. Experimental

2.1. Materials

The PAI was 30% solid suspension in xylene supplied by P.D. George (Tritherm A 981-M-30). The MMT used was Cloisite 20A obtained from Southern Clay Products supplied MMT. All MMT weight fractions reported are based on solid weight content of PAI in the suspension.

2.2. Sample preparation

PAI + MMT nanocomposites were prepared by solvent casting. Silicone molds of known size and shape were prepared. The clay was premixed with xylene for 1 h to improve its swelling capacity. This premix was added very slowly into the PAI suspension with concurrent stirring. The suspension was stirred continuously with the help of a torque controlled Calframo BDC 1850 digital mechanical stirrer with a step wise increase in stirring speeds ranging from 50 to 1000 rpm. The schedule followed was 200 rpm for 5 s, 50 rpm for 20 s, 70 rpm for 90 s, and 1000 rpm for 10 s. This schedule was based on recording optimum conditions for obtaining non-aggregated films using a photoresist spinner. The fragility and brittle nature of the films made removal from the substrate difficult, so we switched to controlled torque mixing followed by casting in silicon molds technique. The high revolutions per minute prevented the flocculation of clay particles. PAI suspension was a mixture of PAI oligomer plus four different aromatic solvents. Selective solvent evaporation technique was therefore used to decrease the effect of trapping the solvents and air. Samples were cured in a mechanical convection oven between 30 and 175 °C. The temperature of the oven was raised by 10 °C after every one and a half hour until final temperature was reached.

Five different compositions (1.0, 1.5, 2.0, 2.5, and 3.0%) MMT by weight of PAI were prepared. Thin films of uniform thickness were used for XRD, OM, SEM, and hardness testing. Thin sections of bulk samples were used for TEM. All error bars are reflective of the magnitude of the standard deviation.

2.3. Polarizing optical microscopy

OM was conducted on a Zeiss polarizing optical microscope. The lens magnification was 40×. The pictures were taken using a CONTAX camera.

2.4. X-ray diffraction

A Siemens D500 X-ray Diffractometer was used to study the diffraction behavior of clay composites. All the experiments were carried out with 2θ varying between 2 and 40°. The scanning speed was 1°/min and the step size was 0.05°. Thin film samples of average thickness equal to 400–500 μm were used. Experiments were carried out at room temperature.

2.5. Transmission electron microscopy

The TEM study was conducted on a JEOL JEM-100CX II electron microscope. A MT6000 Sorvall microtome was

used to cut thin sections (less than 100 nm thick) of the sample.

2.6. Differential scanning calorimetry

DSC data was obtained on a Perkin–Elmer DSC 6 instrument. The system was calibrated using elemental indium. For each run 5–12 mg of sample was used. A first heating run was carried from 30 to 400 °C at a heating rate of 10 °C/min. The sample was held at 400 °C for 5 min and then cooled to 30 °C at a cooling rate of 10 °C/min. The second scan was from 30 to 400 °C at a heating rate of 10 °C/min.

2.7. Thermogravimetric analysis

TGA was performed on Perkin–Elmer TGA instrument. The experiments were carried out from 50 to 1000 °C at a scanning rate of 20 °C/min. The experiments were performed under an air blanket.

2.8. Microhardness testing

Experiments for microhardness test were carried out on a FM-7 Future Tech Corp. digital, microhardness tester. A constant load of 300 g was applied. A dwell time of 15 s was chosen for all samples.

3. Results and discussion

3.1. Dispersion of MMT in PAI

The level of distribution of clay platelets in the PAI matrix was first determined using OM. Typically, the determination of an exfoliated nanocomposite has been based on XRD and TEM results. However, as we have previously determined for epoxy–clay nanocomposites, scanning electron microscopy (SEM) and OM have shown that at the *lower magnification* of SEM and OM scales, the exfoliated and intercalated nanocomposites might still show signs of aggregation similar to clay + water suspensions [40–43]. In aggregation, two or more particles clump together, touching only at certain points. Two states of aggregation are common in montmorillonite layered silicate (MLS)–water suspensions. Coagulation refers to dense aggregates produced by face–face oriented particle associations. Flocculation is based on loose aggregates produced by among others, edge–face or edge–edge oriented particle association. Aggregated clays retain their identity but move kinetically as a single unit [44]. The state of aggregation is driven by heterogeneous charge distribution in natural occurring clays and leads to a number of particle interaction orientations in clay suspensions. Clay suspensions have shown many dispersions including: dispersed; face–face coagulated tactoids, edge–face flocculated, edge–edge flocculated and coagulated particles. The state of aggregation hinders realization of uniform barrier properties. OM images are shown in Fig. 1 for the 1% MMT by weight sample and in Fig. 2 for the MMT by weight 2.5% sample. With increasing clay concentration, the average clay agglomerate size was affected. The average agglomerate size were observed to be around 3.2, 5.0, 5.7, 7.4, and 8.1 μm for 1.0, 1.5, 2.0, 2.5, and 3.0% MMT by weight nanocomposites, respectively. As can be seen, the average platelet size ranged from 3 to 8 μm as the concentration of clay increased. As clay concentration increased the average agglomerate separation of 12, 9, 8, 6, and 5 μm was observed for 1.0, 1.5, 2.0, 2.5, and 3.0% MMT by weight nanocomposites, respectively. As has been shown for clay + water mixtures, when clay is dispersed in aqueous medium of near neutral to alkaline pH, the particles carry a net negative charge, largely due to isomorphic substitution of cations of lower charge for cations of higher charge (Al^{+3} for Si^{+4} in the tetrahedral sheet and Fe^{+2} or Mg^{+2} for Al^{+3} in the octahedral sheet). Meanwhile the clay edges may carry a positive charge in near neutral to acid pH solution because of protonation of various atoms exposed at the edges. We surmise that in a solvent + polymer suspension, charge migration is facilitated through the aqueous medium. We have elsewhere determined increased ionic conductivity with increasing clay content in the solutions [45]. Accurate and reproducible AC impedance measurements of the cast film have not been possible for these systems.

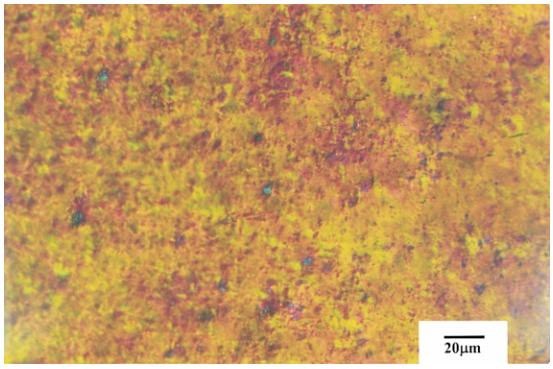

Fig. 1. Optical micrograph of 1.0% PAI nanocomposite showing clay dispersed within PAI matrix.

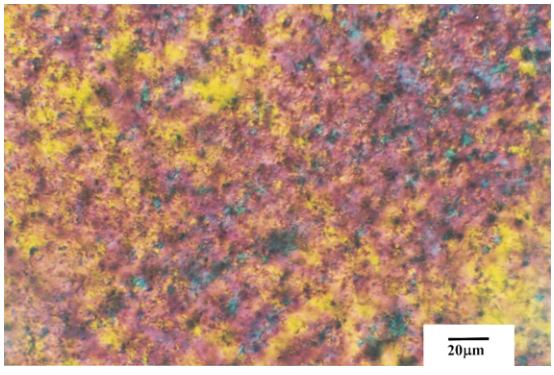

Fig. 2. Optical micrograph of 3.0% PAI nanocomposite showing clay agglomerates that are dispersed in PAI matrix.

XRD was used to characterize the crystallographic structure of MMT. MMT is a layered silicate with an interlayer spacing around 10 Å. The organophilically treated MMT has two characteristic peaks at low 2θ equal to 7.1 and 3.5° (001). The peak at 7.1° corresponds to a basal spacing of 12 Å and the peak at 3.5° corresponds to a basal spacing of 25 Å. Two states of dispersion are obtained when MMT swells due to secondary component migration. When the basal spacing increases and the order is retained, an intercalated composite is obtained. Absence of diffraction peaks corresponding to the interlayer basal spacing is indicative of the disruption of ordered platelet separation leading to an exfoliated dispersion [12,14,16,21,23]. Fig. 3 is a XRD pattern of MMT, blank PAI, 1.0, 1.5, 2.0, 2.5, and 3.0% MMT by weight nanocomposites. As shown in Fig. 3, PAI + MMT nanocomposites containing 1.0% MMT (based on solid weight content of PAI) show no XRD peak corresponding to the interlayer basal spacing. The disruption of the ordered MMT is indicative of an exfoliated dispersion. As shown in Fig. 3 a shift and intense reflections were observed for 1.5 and 2.0% composites. These intense reflections indicate high structural regularity [14]. Here *d* spacings of 32 and 38 Å were observed with respect to clay *d* spacing of 25 Å. Thus, we have an increase in interlayer spacing of 7 Å for 1.5% and 13 Å for 2.0% composite. Fig. 3 shows a similar increase in *d* spacing to 38.48 Å for 2.5% and 38.46 Å for 3.0% composite. For the 3% system however, some minor reflections corresponding to the original *d* spacing are evident. A small fraction of clay does not get intercalated but retains its own identity. Thus, a fraction of MMT is neither intercalated nor exfoliated but forms an immiscible or macro system.

To summarize, the results *based solely on XRD* show a concentration dependent dispersion in the PAI nanocomposite system. An exfoliated dispersion was observed at (1.0%) low clay concentration. Increase in clay concentration from 1.5 to 3.0% resulted in an intercalated dispersion. At low clay concentration, polymer clay interactions overcame the van der Waals forces between silicate galleries resulting in complete disruption of clay structure. Due to an increase in clay concentration, van der Waals interaction dominated polymer clay interactions resulting in a finite expansion of silicate galleries and retention of clay structure. We reached a critical concentration of 1.5 and 2.0% composite where high structural intercalation was observed. Even though the *d* spacing increased to ~38 Å, 2.5 and 3.0% showed partial intercalation and exfoliation.

The state of exfoliation and intercalation inferred from XRD was further analyzed by TEM. A transmission electron micrograph of a 1.0% clay nanocomposite is shown in Fig. 4. Individual crystallites of the silicate are visible as regions of alternating narrow, dark and light bands within the particle. The face–edge connectivity of the platelets is a further proof of charge mediated clay–clay attraction influencing the system. Fig. 4 shows a disruption of ordered platelet with an average platelet separation (determined using NIH-Image) of 28 nm. This is an indication of a dominating exfoliated dispersion. The dark lines are the cross-section of face–face coagulated dispersions. These dark lines have variable thickness from 10 to 30 Å. This variable thickness is due to stack of silicate layers one above each other thus indicating that *even in a highly exfoliated nanocomposite*, *significant layer stacking* occurs. TEM of the 3% nanocomposite shows high level of stacking but also large areas of matrix rich material (Fig. 5). The average platelet separation for 1.0, 1.5, 2.0, 2.5, and 3.0% MMT by weight nanocomposites were found to be 28, 9, 12, 11, 8, respectively. This indicates that XRD and TEM should not just be interpreted for clay stacking or dispersions but for the possibility of phase separation of clay tactoids leading to matrix dominant areas. The trend in platelet spacings indicated by TEM confirmed XRD results. Wider platelet separation was

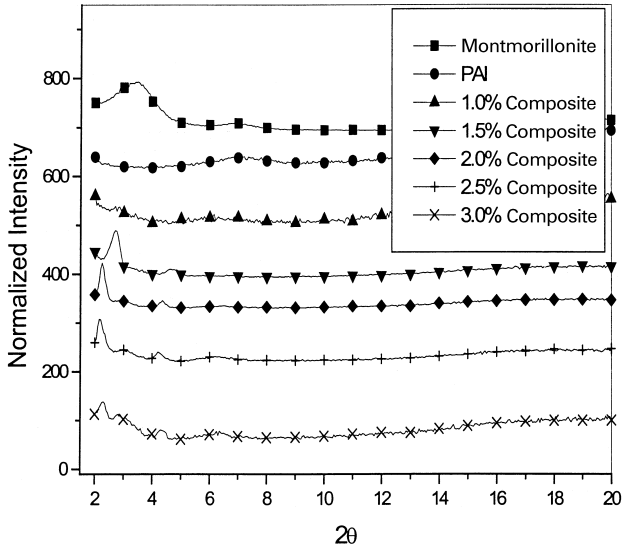

Fig. 3. XRD of MMT and its nanocomposites.

Fig. 4. TEM of a 1% PAI nanocomposite showing face–face coagulation, edge–edge flocculated tactoids in an exfoliated nanocomposite.

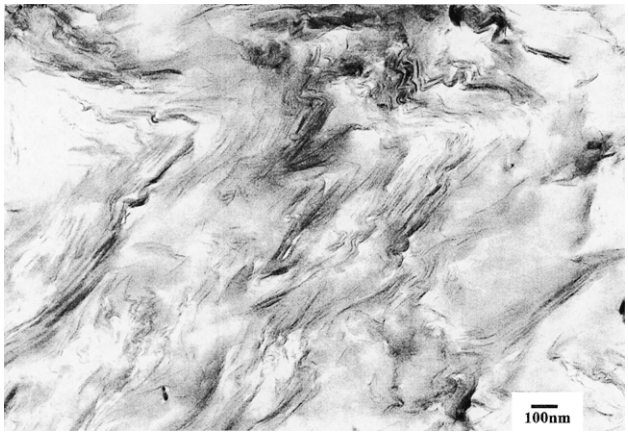

Fig. 5. TEM of 2.5.0% PAI nanocomposite showing high level of matrix rich areas.

observed for the exfoliated (1.0%) dispersion. Clay composites of 1.5–3.0% showed separations from 8 to 12 nm indicating an intercalated dispersion. This occurrence of both intercalation and exfoliation is not predicted by molecular modeling based on purely thermodynamic considerations [46–51]. However, these results and those by others on the influence of molecular weight and mechanical shear on intercalation and exfoliated dispersions, indicates that kinetic effects determine the final dispersion of a polymer nanocomposite [52]. Even when the repeat unit of the polymer is the same, two dispersions can exist based on concentration of the clay.

3.2. Thermal behavior

Fig. 6 shows the first and second heating thermograms of the samples. As can be seen, in the first heat both PAI and montmorillonite have volatile emissions. For montmorillonite Xie et al. [53] conducted a detailed analysis of evolution of volatiles in organically modified montmorillonite. For temperatures between 200 and 500 °C organics, CO_2 and long chain alkyl fragments are detected. However, in the same regime, remnant volatiles from the PAI suspension are also evolved making assignment of peaks difficult. To validate analysis of the second heat and to determine if the PAI was affected by the surfactant degradation, FTIR was conducted on samples before and after being subjected to 1 h at 400°. The results are shown in Fig. 7. As can be seen no degradation of PAI was evident for all the samples.

We examined our results of the second heating thermogram in the context of results and reviews by McKenna on controlled pore geometries [54–58]. For controlled pore geometries, he determined two glass transitions related to the liquid plug at the core and an interacting surface layer [54]. A hump in the specific heat plots was indicative of material not confined to the pores. The influence of solvent elution and its influence on the generation of two glass transitions has also been reviewed [59]. The presence of two glass transitions has been investigated by Tsagaropoulos and Eisenberg [60] for the general case of filled polymers indicating that the presence of fillers and possible matrix constraint is reflected by two glass transitions. As shown in Fig. 8, there was only one T_g in all systems but a hump observable just after the transition, indicates the presence of material that is not confined between the clay. This is supported by the TEM images in Figs. 4 and 5 where substantial areas indicate clay poor and polymer rich regions. The absence of two glass transitions is indicative that the polymer either does not have different relaxations near the reinforcement than away from it or that the technique of DSC has not been sensitive to the minor relaxation. We postulate that the degree of tactoid formation, micron dimensions of the tactoids and the ability of these tactoids to move kinetically as one leads to a state of macroreinforcement when nanocomposites are formed from

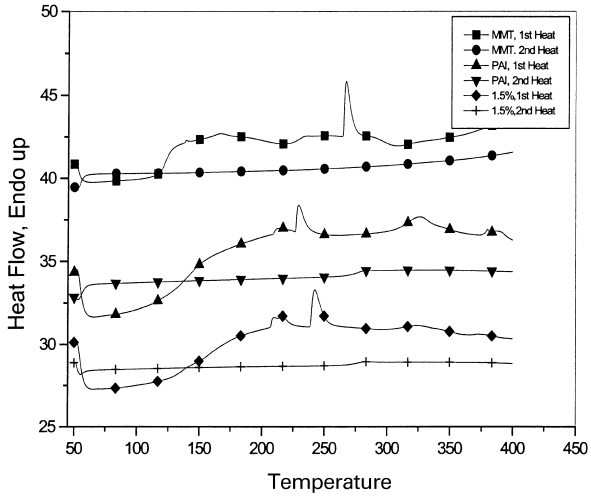

Fig. 6. First and second heat DSC thermograms showing PAI solvent and organic surfactant tethered to montmorillonite emissions.

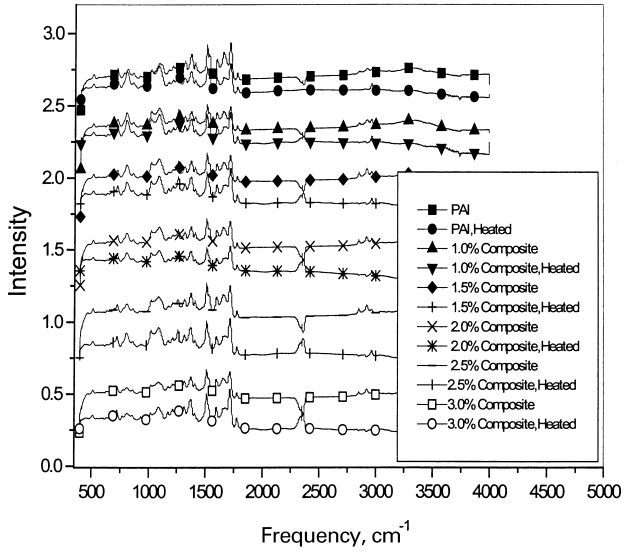

Fig. 7. FTIR of PAI and the nanocomposites showing no change in PAI spectra due to surfactant degradation.

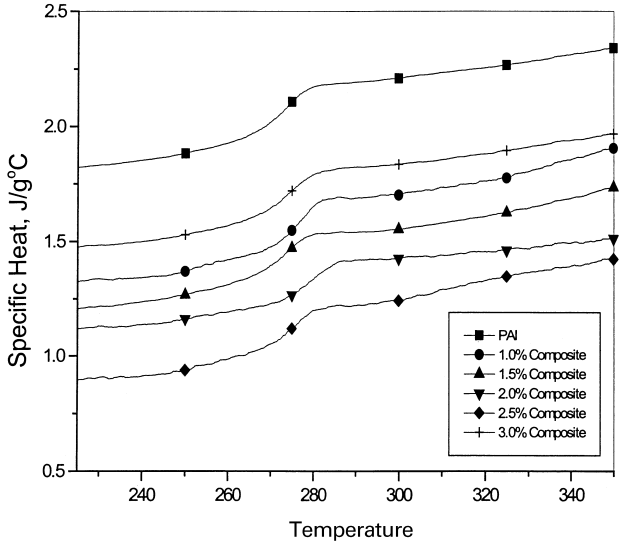

Fig. 8. Specific heat—temperature profiles of the second heat showing no change in glass transition or width of the transition with concentration.

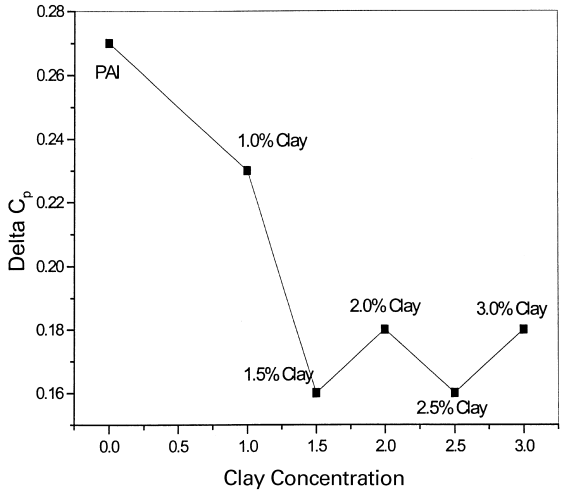

Fig. 9. ΔC_p changes as a function of concentration showing a decrease for all nanocomposites where XRD shows a 001 clay peak.

solution or in mobile media. We point to our prior work in epoxy systems [40,43,61] where SEM of the through thickness cross-sections showed that even though XRD and TEM indicated exfoliated systems, at the macroscale clay aggregates existed of these 'exfoliated' and 'intercalated' dispersions. The contribution of the matrix characteristics to this would be both in terms of mobility and charge transport characteristics. The solution viscosity and static state of the suspension during curing or solvent removal would aid re-aggregation of the sheared clay platelets. Further, the charge transport capability of the polymer would facilitate the aggregation of the charged platelets. We point out the increased interest in montmorillonite + polyethylene oxide combinations for solid fuel cell applications. In parallel work with melt processed polypropylene we see no sign of this macroaggregated state [62]. We have attributed this to the high viscosity of the melt and continuous high shear in injection molding samples.

We examined the change in specific heat across the transition (Fig. 9) and determined a slight decrease in the specific heat for the primarily exfoliated nanocomposite. However all highly intercalated systems showed a much lower specific heat change. The breadth of the transition is not affected by the dispersion or change in concentration.

The thermogravimetric data was analyzed to determine if the surfactant degradation was influenced by type of dispersion. As shown in Fig. 10, PAI, 1.5 and 2% samples have similar degradation profiles that are not affected by the montmorillonite surfactant degradation. For the highly exfoliated 1%, and minimally intercalated 2.5 and 3% samples the curves are closer to the organically modified montmorillonite. Thus, we can speculate that interacting polymer chains between the clay layers serve not just to shield the polymer as typically inferred but rather is influenced by level of intercalation. For a highly intercalated material, the increased solvation between the chains and the end-tethered alkyl ammonium group ensures protection from the alkyl ammonium degradation with the clay acting as barriers for thermooxidative stability.

3.3. Mechanical properties

Fig. 11 shows the Vickers hardness of PAI and PAI + MMT nanocomposites of different MMT concentration. Addition of MMT showed a marked increase in hardness of around 32%. At 1.0%, which showed exfoliated dispersion, the highest hardness was observed. The uniformly distributed exfoliated platelets improved the stiffness of PAI. Presence of these stiff clay platelets and entanglement of polymer chains made the PAI nanocomposite harder. The intercalated dispersions showed almost similar hardness where polymer chains are penetrated into silicate galleries.

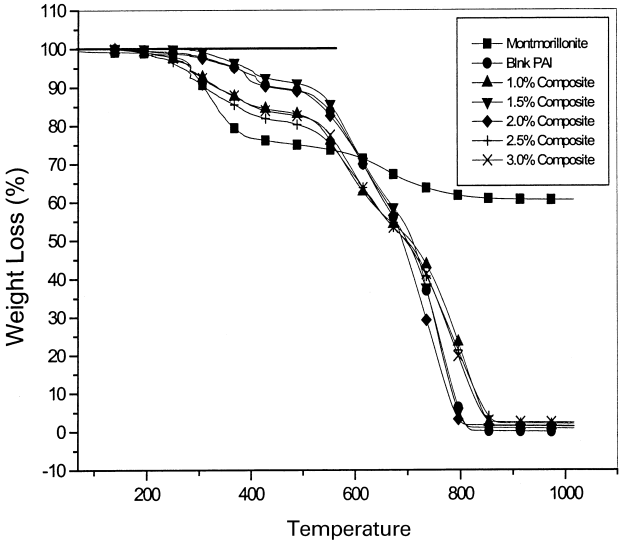

Fig. 10. Thermogravimetric curves for montmorillonite, blank PAI and PAI nanocomposites.

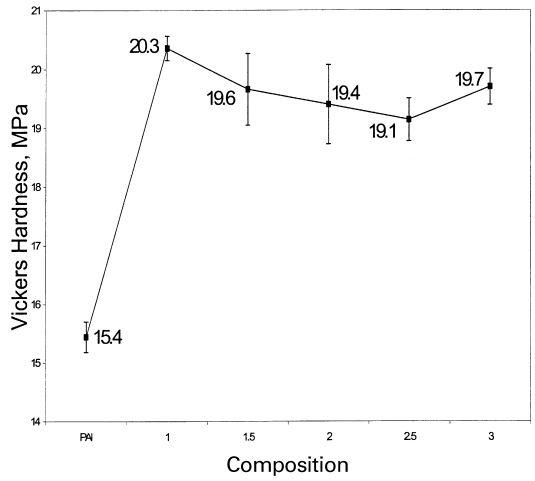

Fig. 11. Vickers hardness of PAI and PAI + MMT nanocomposites.

Finite penetration of polymer chains did not improve the hardness of PAI over that of the 1.0% PAI nanocomposite, mainly due to retention of clay structure. The addition of MMT increased the hardness of PAI from 15 to 20 MPa. Dispersion dependent mechanical properties were obtained where the exfoliated dispersion showed the highest hardness compared to the intercalated dispersion.

4. Conclusions

A mixed intercalated and exfoliated system of PAI and clay was developed. In contrast to the clear intercalated and exfoliated interpretations of XRD spectra, TEM showed significant layer or platelet stacking. The trends of average platelet to platelet separation distances however mirrored that of XRD. The results present evidence that even though the concentration of clay increased, the higher face–face coagulated state with concentration led to more matrix rich areas. The presence of mixed exfoliated and intercalated state for the same system highlights the kinetic influences on the dispersion of clay layers into polymers. This is especially true in in-situ approaches or in solution processing where the removal of solvent introduces a finite rate effect on the equilibrium configuration of the plate like morphology of the clay layers. The glass transition temperature was not significantly affected by the presence of clay though the change in specific heat for the glass transition decreased with increasing clay concentration.

Analysis of the DSC thermograms in conjunction with the FTIR of heat treated samples indicated that solvent evaporation from the PAI and clay surfactant degradation did not affect the PAI structure. The amount of weight loss associated with these transitions was however found to be dispersion dependent. The presence of clay resulted in increased hardness but this was concentration independent.

Acknowledgements

We gratefully acknowledge Doug Hunter, Southern Clay Products for recommendations on clay selection as well as materials. Advice from the reviewers and Lars Berglund, Lulea University is gratefully acknowledged. Instrumentation assistance from Kevin Menard, Perkin Elmer, Witold Brostow, David Garrett, W.E. Acree, Teresa D. Golden and Jason Griggs is appreciated. We also acknowledge J. Yodis and S. George, for the Polyamide-imide suspension. Financial support from the Texas Advanced Technology Program Grant 003656-0037b is acknowledged.

References

[1] Kojima Y, Fukumori K, Usuki A, Okada A, Kurauchi T. J Mater Sci Lett 1993;12:889.
[2] Kojima Y, Usuki A, Kawasumi M, Okada A, Fukushima Y, Kurauchi T, Kamigaito O. J Mater Res 1993;8(5):1185.
[3] Kurokawa Y, Yasuda H, Kashiwagi M, Oyo A. J Mater Sci Lett 1997;16:1670.
[4] Yano K, Usuki A, Okada A, Kurauchi T, Kamigaito O. J Polym Sci 1993;31:2493.
[5] Usuki A, Kojima Y, Kawasumi M, Okada A, Fukushima Y, Kurauchi T, Kamigaito O. J Mater Res 1993;8(5):1179.
[6] Usuki A, Kojima Y, Kawasumi M, Okada A, Fukushima Y, Kurauchi T, Kamigaito O. J Mater Res 1993;8(5):1174.
[7] Kojima Y, Usuki A, Kawasumi M, Okada A, Kurauchi T, Kamigaito O. J Polym Sci 1993;31:983.
[8] Kojima Y, Usuki A, Kawasumi M, Okada A, Kurauchi O, Kamigaito O, Kaji K. J Polym Sci 1994;32:625.
[9] Kojima Y, Matsuoka T, Iakahashi H, Kurauchi T. J Appl Polym Sci 1994;51:683.
[10] Bidadi H, Schroeder PA, Pinnavaia TJ. J Phys Chem Solids 1998;49(12):1435.
[11] Krishnamoorti R, Giannelis EP. Macromolecules 30: 4097.
[12] Giannelis EP. Adv Mater 1996;8(1):29.
[13] Burnside SD, Giannelis EP. Chem Mater 1995;7(9):1597.
[14] Vaia RA. Polymer melt intercalation in mica-type layered silicates. PhD Thesis. USA: Cornell University, May, 1995.
[15] Krishnamoorti R, Vaia RA, Giannelis EP. Chem Mater 1996;8:1728.
[16] Vaia RA, Sauer BB, Tse OK, Giannelis EP. J Polym Sci 1997;35:59.
[17] Vaia RA, Vasudevan S, Krawiec W, Scanlan LG, Giannelis EP. Adv Mater 1995;7(2):154.
[18] Vaia RA, Jandt KD, Kramer EJ, Giannelis EP. Chem Mater 1996;8:2628.
[19] Vaia RA, Giannelis EP. Macromolecules 1997;30:8000.
[20] Vaia RA, Giannelis EP. Macromolecules 1997;30:7990.
[21] Wang Z, Pinnavaia TJ. Chem Mater 1998;10:1820.
[22] Wang MS, Pinnavaia TJ. Chem Mater 1994;6:468.
[23] Lan T, Kaviratna PD, Pinnavaia TJ. J Phys Chem Solids 1996;57:1005.
[24] Kaviratna PD, Pinnavaia TJ, Schroeder PA. J Phys Chem Solids 1996;57(12):1897.
[25] Messersmith PB, Giannelis EP. J Polym Sci 1995;33:1047.
[26] Lan T, Pinnavaia TJ. Chem Mater 1994;6:2216.
[27] Wang Z, Pinnavaia TJ. Chem Mater 1998;10:3769.
[28] Lan T, Kaviratna PD, Pinnavaia TJ. Chem Mater 1994;6:573.
[29] Lan T, Kaviratna PD, Pinnavaia TJ. Chem Mater 1995;7:2144.
[30] Giannelis EP. J Miner 1992;44(3):28.
[31] Messersmith PB, Giannelis EP. Chem Mater 1994;6:1719.
[32] Dagani R. Chem Engng News 1999;77(23):25.
[33] Miller B. Plast Formulating Compound 1997;May/June:30.

[34] Sherman LM. Plast Technol 1999;June:52.
[35] Shen Z. Nanocomposites of polymers and layered silicates. PhD Thesis. Australia: Monash University, October, 2000.
[36] Kornmann X, Lindberg H, Berglund LA. Polymer 2001;42:1303.
[37] Burnside SD, Wang HC, Giannelis EP. Chem Mater 1999;11:1055.
[38] Giannelis EP. Chem Mater 1990;2:627.
[39] Messersmith PB, Giannelis EP. Chem Mater 1993;5:1064.
[40] Butzloff P. Master's Thesis. University of North Texas, December, 2000.
[41] Butzloff P, D'Souza NA. Annual Technical Conference of the Society of Plastics Engineers, 2000. p. 1527.
[42] Butzloff P, D'Souza NA. Annual Technical Conference of the Society of Plastics Engineers, 2000. p. 1531.
[43] Butzloff P, D'Souza NA, Golden TD, Garrett D. Polym Engng Sci 2001;41:1794.
[44] Schramm LL. In: Schramm LL, editor. Suspensions: fundamentals and applications in the petroleum industry. Washington, DC: American Chemical Society, 1996.
[45] Ranade A. Exfoliated and intercalated polyamide-imide nanocomposites. MS Thesis. University of North Texas, 2001.
[46] Vaia RA. Polymer melt intercalation in mica-type layered silicates. PhD Thesis. USA: Cornell University, May, 1995.
[47] Vaia RA, Sauer BB, Tse OK, Giannelis EP. J Polym Sci 1997;35:59.
[48] Vaia RA, Vasudevan S, Krawiec W, Scanlan LG, Giannelis EP. Adv Mater 1995;7:154.
[49] Vaia RA, Jandt KD, Kramer EJ, Giannelis EP. Macromolecules 1995;28:8080.
[50] Vaia RA, Giannelis EP. Macromolecules 1997;30:8000.
[51] Vaia RA, Giannelis EP. Macromolecules 1997;30:7990.
[52] Fornes TD, Yoon PJ, Keskkula H, Paul DR. Polymer 2001;42:9929.
[53] Xie W, Gao Z, Pan W, Vaia R, Hunter D, Singh A. Thermochim Acta 2001;367–368:339.
[54] Park JY, McKenna GB. Phys Rev B 2000;61:6667.
[55] McKenna GB. Conference Proceedings ANTEC. vol. II, 2000. p. 2004.
[56] McKenna GB. J Phys IV France 2000;10:7–343.
[57] Jackson CL, McKenna GB. Chem Mater 1996;8:2128.
[58] McKenna GB. J Phys IV France 2000;10:7–53.
[59] Tsui OKC, Russsell TP, Hawker CJ. Macromolecules 2001;34:5535.
[60] Tsagouropolos G, Eisenberg A. Macromolecules 1995;28:6067.
[61] Butzloff P, D'Souza NA. Submitted for publication.
[62] Hernandez-Luna A, D'Souza NA, Ranade A, Drewniak M. Annual Technical Conference for the Society of Plastics Engineers, 2002. Accepted for publication.